MOX–Report No. 16/2008

Numerical simulation of the dynamics of boat by a variational inequality approach

Luca Formaggia, Edie Miglio,
Andrea Mola, Anna Scotti

MOX, Dipartimento di Matematica "F. Brioschi"
Politecnico di Milano, Via Bonardi 29 - 20133 Milano (Italy)

mox@mate.polimi.it http://mox.polimi.it

Numerical simulation of the dynamics of boats by a variational inequality approach

L. Formaggia♯, E. Miglio♯, A. Mola♯ and A. Scotti♯

July 11, 2008

♯ MOX– Modellistica e Calcolo Scientifico
Dipartimento di Matematica "F. Brioschi"
Politecnico di Milano
via Bonardi 9, 20133 Milano, Italy
luca.formaggia@polimi.it,edie.miglio@polimi.it,
andrea.mola@polimi.it, anna.scotti@mail.polimi.it

Keywords:Computational Fluid Dynamics, Fluid structure interaction, Variational Inequalities, Dynamics of rowing

AMS Subject Classification: 76D33, 74F10, 76B07, 76B20, 65N30, 47J30

Abstract

In this paper we present some recent numerical studies on fluid-structure interaction problems in the presence of free surface flow. We consider the dynamics of a rowing boat, simulated as a rigid body. We focus on an approach based on formulating the floating body problem as an inequality constraint on the water elevation. A splitting procedure is used to develop an efficient numerical scheme where the inequality constraint is imposed only on a wave like equation representing an hydrostatic approximation of the hydrodynamic equations. Numerical tests demostrate the effectiveness of the proposed procedure.

1 Introduction

The use of computational fluid dynamics (CFD) in boat design is traditionally based on potential flow theory, even if in the last years the use of Reynolds Averaged Navier-Stokes (RANS) codes has become increasingly more common. The role of CFD is of particular importance whenever performance optimisation is critical, such as in competition boats, where even a small advantage may be crucial. An overview on the numerical techniques

for ship hydrodynamics may be found in [5, 4] and, more specifically, their relevance for high performance sailing boat in [14].

In this field, most of the numerical investigations aim to assess the boat characteristics at a given fixed configuration. Furthermore, they usually compute a steady state solution, even if sometimes this is reached through pseudo time stepping. Yet, simulating the full dynamics of a boat may be of great importance [1, 15]. We mention two cases: high performance sailing boats and rowing sculls. In the former, the accurate simulation of the dynamics may allow for a better trimming of the boat [1, 16], better evaluating wave resistance [13] and in perspective the assessment of its performance during manoeuvring. For a competition rowing scull, accounting for the dynamics effects is even more important. Indeed, because of the periodic action at the oars and the movement of the oarsmen on the boat the motions of the scull is very complex and characterised by horizontal accelerations/decelerations, sinking and dipping. These secondary movements generate waves which dissipate part of rowers energy, which could be better spent to move the boat forward.

In this paper, we will give an account of some current research in this class of problems by focusing on a numerical model based on the solution of quasi-3D Navier-Stokes equations with free surface [11], where the presence of the boat is modelled through an inequality constraint. We show how the method is able to reproduce the general wave patterns of a moving scull.

2 A variational approach to the floating body problem

We will consider the free-surface Navier-Stokes equations where part of the surface is subject to a constraint which is meant to represents the external surface of a boat. More precisely, we will consider for any $t \in (0, T)$, with $T > 0$, the domain

$$\Omega(t) = \{(\boldsymbol{x} = (x, y, z) \in \mathbb{R}^3 : \, (x, y) \in \omega, z \in (-h, \eta(x, y, t))\}$$

sketched in Fig. 1 is occupied by a fluid, being η the description of the free surface of the fluid (measured with respect to the unperturbed water depth). The part of the boundary of Ω corresponding to the free surface is denoted by

$$\Gamma_s(t) = \{\boldsymbol{x} \in \mathbb{R}^3 : \, (x, y) \in \omega, \, z = \eta(x, y, t)\}.$$

Here, ω is an open bounded connected subset of $\mathbb{R}^2$ and we are implicitly assuming that the free surface can be represented by a function of (x, y), i.e no wave breaking occurs during the motion. The bottom surface is

$$\Gamma_b = \{\boldsymbol{x} \in \mathbb{R}^3 : \, (x, y) \in \omega, \, z = -h\},$$

where h indicates the depth of the bottom surface (again measured with respect to the unperturbed water level) which, for the sake of simplicity, is assumed to be constant. The remaining portion of $\partial\Omega(t)$ is the far field

$$\Gamma_f(t) = \{\boldsymbol{x} \in \mathbb{R}^3 : (x, y) \in \partial\omega,\ z \in (-h, \eta(x, y, t))\}.$$

Clearly, $\partial\Omega(t) = \bar{\Gamma}_s(t) \cup \bar{\Gamma}_b \cup \bar{\Gamma}_f(t))$ at any time t.

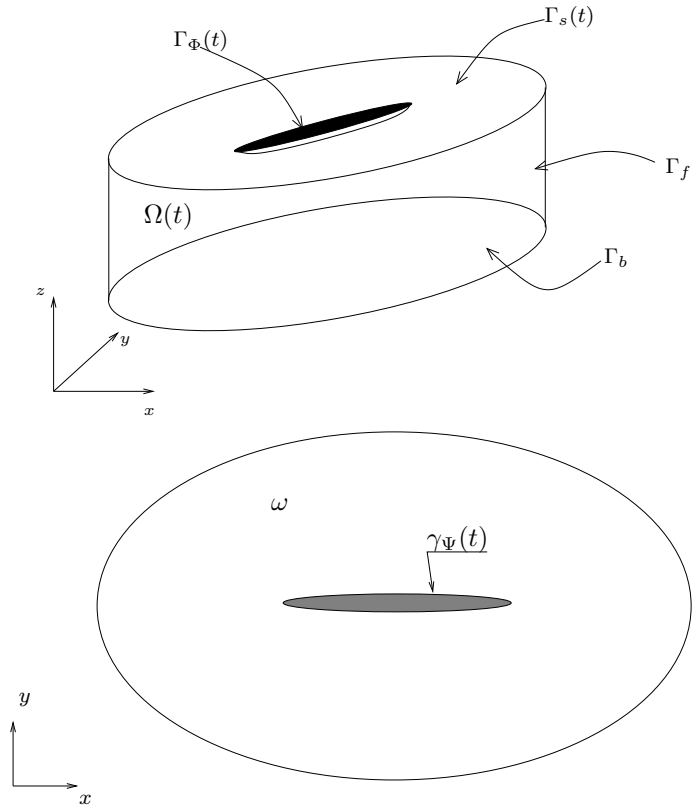

Figure 1: The 3D computational domain (top) and its projection on the horizontal plane ω (bottom). The shadowed figure in the bottom picture represents the projection of the immersed part of the boat on the fluid surface, it is then part of ω.

We now consider a continuous function

$$\Psi : \omega \times [0, T] \to \mathbb{R} \tag{1}$$

which is meant to represent the external surface of the hull of a boat, suitably extended to cover all ω (see Fig.2). We want to simulate the presence of a floating boat by constraining the free surface η to be at any time below Ψ. The evolution of Ψ will be normally given by the interaction of the fluid

with the floating boat, yet in the following we assume that Ψ is given and that the (possibly empty) set

$$\gamma_\Psi(t) = \{(x, y) \in \omega : \Psi(x, y, t) = \eta(x, y, t)\} \tag{2}$$

is always strictly included in ω for all $t \in [0, T]$. This is clearly an "a-priori" assumption, since η is one of our unknowns (and also Ψ when is obtained from the solution of a fluid-structure interaction problem). Yet, for many practical situations it is fulfilled whenever Ψ and ω are properly chosen.

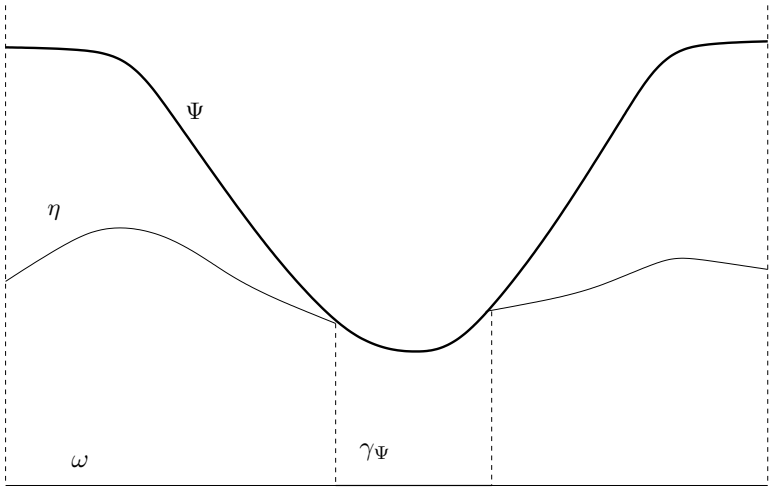

Figure 2: A two dimensional view of the constrained problem. η is constrained to remain below Ψ at any time.

In our case, $\gamma_\Psi(t)$ will denote the horizontal projection of the "submerged surface" of the boat

$$\Gamma_\Psi(t) = \{(x, y) \in \gamma_\Psi(t),\ z = \Psi(x, y, t)\},$$

while $\boldsymbol{U}$ and p denote the velocity and the pressure (scaled with the density), respectively. If $D = \{(\boldsymbol{x}, t) : t \in (0, T),\ \boldsymbol{x} \in \Omega(t)\}$ we have that $\boldsymbol{U} : D \to \mathbb{R}^3$ and $p : D \to \mathbb{R}$.

Furthermore, we put into evidence the x and y components of the velocity by writing

$$\boldsymbol{U} = (\boldsymbol{u}, w) = (u_x, u_y, w),$$

and indicating by $\boldsymbol{\nabla}_{xy}$ and div_{xy} the gradient and the divergence operator in the (x, y) plane, respectively. The flow equations governing this problem may be conveniently written by introducing a Lagrange multiplier $\lambda : \omega \times (0, T) \to \mathbb{R}_+$ and solving for a.o. $t \in (0, T)$, the following system for the

unknown $\boldsymbol{U}$, p, η and λ,

$$\begin{array}{ll} \dfrac{D\boldsymbol{U}}{Dt} + \mathbf{div}\boldsymbol{\sigma}(\boldsymbol{U}) + \boldsymbol{\nabla} p - \boldsymbol{g} = \mathbf{0} & \text{in } \Omega(t), \\ \operatorname{div} \boldsymbol{U} = 0 & \\ \dfrac{\partial \eta}{\partial t} + u_x \dfrac{\partial \eta}{\partial x} + u_y \dfrac{\partial \eta}{\partial y} - w = 0 & \text{in } \omega. \\ \lambda(\eta - \Psi) = 0, \quad \lambda \geq 0, \quad \eta - \Psi \leq 0 & \end{array} \tag{3}$$

with the additional dynamic condition

$$(\sigma(\boldsymbol{U}) + p\boldsymbol{I}) \cdot \boldsymbol{n} - \lambda \boldsymbol{n} = 0, \quad \text{on } \Gamma_s(t), \tag{4}$$

being $\boldsymbol{n}$ the outward normal of $\partial\Omega(t)$. This condition implies that the external pressure acting on the free surface $\Gamma_s(t) \setminus \Gamma_\Psi(t)$ is constant and equal to zero.

Here, $\boldsymbol{g} = -g\boldsymbol{e}_z$ is the gravity acceleration, while $\boldsymbol{\sigma}$ denotes the viscous contribution to the internal stress, which in our case may be taken equal to $\boldsymbol{\sigma}(\boldsymbol{U}) = -\nu\boldsymbol{\nabla}\boldsymbol{U}$, being ν the water kinematic viscosity, assumed constant. We have indicated by $\dfrac{D\boldsymbol{U}}{Dt} = \dfrac{\partial \boldsymbol{U}}{\partial t} + (\boldsymbol{U} \cdot \boldsymbol{\nabla})\boldsymbol{U}$ the material derivative. In deriving the first two equations in (3) we have assumed that the water density ρ is constant, and we have eliminated it from the equations by scaling. Let us note that the support of $\lambda(t)$ is always contained in $\gamma_\Psi(t)$.

System (3) has to be complemented with proper boundary conditions on $\Gamma_f(t)$ and Γ_b, which will be detailed later on, as well as initial conditions on $\boldsymbol{U}$ and η.

We now exploit the special shape of the domain to operate on (3). First, we decompose the pressure as

$$p(\mathbf{x}, t) = g(\eta(x, y, t) - z) + q(\mathbf{x}, t) + \lambda(\mathbf{x}, t), \tag{5}$$

where q is the so called "hydrodynamic correction" (see [11]), while $g(\eta - z)$ is the hydrostatic part.

Furthermore, we integrate the continuity equation along the z direction by imposing $\boldsymbol{U} \cdot \boldsymbol{n} = 0$ on Γ_b and exploiting the kinematic interface condition, to obtain

$$\begin{array}{ll} \dfrac{D\boldsymbol{u}}{Dt} - \nu\triangle\boldsymbol{u} + g\boldsymbol{\nabla}_{xy}\eta - \nu\dfrac{\partial \boldsymbol{u}}{\partial z} + \boldsymbol{\nabla}_{xy}\lambda + \boldsymbol{\nabla}_{xy} q = \mathbf{0} & \\ \dfrac{Dw}{Dt} - \nu\triangle w + \dfrac{\partial q}{\partial z} = 0 & \text{in } \Omega(t), \\ \operatorname{div}_{xy} \boldsymbol{u} + \dfrac{\partial w}{\partial z} = 0 & \\ \dfrac{\partial \eta}{\partial t} + \operatorname{div}_{xy} \displaystyle\int_{-h}^{\eta} \boldsymbol{u}\, dz = 0 & \text{in } \omega. \\ \lambda(\eta - \Psi) = 0, \quad \lambda \geq 0, \quad \eta - \Psi \leq 0 & \end{array} \tag{6}$$

The dynamic condition on $\Gamma_s(t)$ becomes $\sigma(\boldsymbol{U}) \cdot \boldsymbol{n} = \mathbf{0}$, i.e. $\frac{\partial \boldsymbol{U}}{\partial n} = \mathbf{0}$. We have assumed, as usual in this type of derivations, that the dynamic pressure q is zero on $\Gamma_s(t)$. As a result, the Lagrange multiplier λ may be understood as the pressure field exerted on the water surface by the presence of the boat.

We wish now to solve this problem numerically. To this purpose we first reduce it to a simpler problem, more amenable to numerical analysis, by performing the integration in time.

2.1 Characteristic treatment of the time derivative

We subdivide the time interval $[0, T]$ into N sub-intervals of width Δt and we denote with $t^n = n\Delta t$ the n-th time step. The subscript n denotes the approximation at $t = t^n$ of the various time-dependent quantities. The method of characteristics consists in performing the following approximation

$$\frac{D\boldsymbol{U}}{Dt}(\mathbf{x}, t^{n+1}) \simeq \frac{\boldsymbol{U}(\mathbf{x}, t^{n+1}) - \boldsymbol{U}(\mathbf{X}((\mathbf{x}, t^{n+1}; t^n), t^n))}{\Delta t}, \tag{7}$$

where $\mathbf{X}((\mathbf{x}, t^{n+1}; t^n), t^n)$ is obtained by solving the following time backward differential problem for each $\mathbf{x} \in \Omega(t)$,

$$\begin{cases} \dfrac{d\boldsymbol{X}}{d\tau}(\mathbf{x}, t^{n+1}; t^{n+1} - \tau) = -\boldsymbol{U}(\mathbf{X}(\mathbf{x}, t^{n+1}; t^{n+1} - \tau), t^{n+1} - \tau), \quad \tau \in (0, \Delta t), \\ \boldsymbol{X}(\mathbf{x}, t^{n+1}; t^{n+1}) = \mathbf{x}. \end{cases}$$

More details on this technique may be found in [11] or in [3]. We will now use the short hand notation $\mathbf{X}^n$ to indicate $\mathbf{X}((\mathbf{x}, t^{n+1}; t^n), t^n))$ and replace (6) with the approximation

$$\begin{aligned} &\frac{\boldsymbol{u}^{n+1} - \boldsymbol{u}^n(\mathbf{X}^n)}{\Delta t} - \nu \triangle \boldsymbol{u}^{n+1} + g\boldsymbol{\nabla}_{xy}\eta^{n+1} + \boldsymbol{\nabla}_{xy}\lambda^{n+1} + \boldsymbol{\nabla}_{xy}q^{n+1} = \mathbf{0} \\ &\frac{w^{n+1} - w^n(\mathbf{X}^n)}{\Delta t} - \nu \triangle w^{n+1} + \frac{\partial q^{n+1}}{\partial z} = 0 \qquad \text{in } \Omega^{n+1}, \\ &\operatorname{div}_{xy} \boldsymbol{u}^{n+1} + \frac{\partial w^{n+1}}{\partial z} = 0 \\ &\frac{\eta^{n+1} - \eta^n}{\Delta t} + \operatorname{div}_{xy} \int_{-h}^{\eta^{n+1}} \boldsymbol{u}^{n+1}\, dz = 0 \qquad \text{in } \omega, \\ &\lambda^{n+1}(\eta^{n+1} - \Psi^{n+1}) = 0, \quad \lambda \geq 0, \quad \eta^{n+1} - \Psi^{n+1} \leq 0 \end{aligned} \tag{8}$$

where the quantities at time t^n are assumed to be known.

This system of equations can be further modified by adopting an operator splitting strategy analogous to the one employed in the well-known Chorin-Temam scheme [6] for incompressible fluid dynamics. More precisely, we first perform a *hydrostatic step*, which computes an intermediate velocity

field $\tilde{\boldsymbol{u}}$, as well as λ^{n+1} and η^{n+1} by solving the system

$$\begin{aligned}
&\frac{\tilde{\boldsymbol{u}} - \boldsymbol{u}^n(\mathbf{X}^n)}{\Delta t} - \nu\triangle\tilde{\boldsymbol{u}} - \nu\frac{\partial^2\tilde{\boldsymbol{u}}}{\partial z^2} + g\boldsymbol{\nabla}_{xy}\eta^{n+1} + \boldsymbol{\nabla}_{xy}\lambda^{n+1} = \mathbf{0} \quad \text{in } \Omega^{n+1}\\
&\frac{\eta^{n+1}-\eta^n}{\Delta t} + \mathrm{div}_{xy}\int_{-h}^{\eta^{n+1}} \tilde{\boldsymbol{u}}\, dz = 0 \qquad \text{in } \omega,\\
&\lambda^{n+1}(\eta^{n+1} - \Psi^{n+1}) = 0, \quad \lambda \geq 0, \quad \eta^{n+1} - \Psi^{n+1} \leq 0
\end{aligned} \tag{9}$$

followed by a *correction step* for the actual computation of the solution

$$\begin{aligned}
&\frac{\boldsymbol{u}^{n+1} - \tilde{\boldsymbol{u}}}{\Delta t} + \boldsymbol{\nabla}_{xy} q^{n+1} = \mathbf{0}\\
&\mathrm{div}_{xy}\,\boldsymbol{u}^{n+1} + \frac{\partial w^{n+1}}{\partial z} = 0\\
&\frac{w^{n+1} - w^n(\mathbf{X}^n)}{\Delta t} - \nu\triangle w^{n+1} + \frac{\partial q^{n+1}}{\partial z} = 0,
\end{aligned} \tag{10}$$

in Ω^{n+1}.

It is possible to neglect the hydrodynamics pressure term q, using the so-called hydrostatic approximation. In that case we set $q = 0$ everywhere, $\boldsymbol{u}^{n+1} = \tilde{\boldsymbol{u}}$ and we solve only the second equation in (10) to obtain the vertical component of the velocity. Another possible approximation is to neglect the term $-\nu\triangle\tilde{\boldsymbol{u}}$ in the first equation of (9), this has important consequence in the regularity of the solution (see [8] and [9]) and in the numerical scheme.

For what matters at the moment is to notice that with this splitting the unilateral constraint is imposed on a simpler set of equations. We now consider on how to apply the constraint in practise.

2.2 Enforcing the constraint in the hydrostatic step

Let us consider (9) in more detail. We note that the problem is non-linear because the domain Ω^{n+1} is unknown, as it depends on η^{n+1}. In order to avoid a complex iterative procedure, we linearize the problem by computing a first approximation of Ω^{n+1} based on a full explicit treatment of the free surface evolution. In practise, we first solve

$$\eta^* = \eta^n + \Delta t \mathrm{div}_{xy}\int_{-h}^{\eta^n} \boldsymbol{u}^n\, dz$$

and use it for the approximation of the domain at time t^{n+1}. The actual domain at time t^{n+1} will be calculated at the end of the step from the computed values of η^{n+1}. We now rewrite (9) where, for the sake of notation, we drop the superscript $(n+1)$ and the bar, and we set $\alpha = (\Delta t)^{-1}$.

The problem is to find $\boldsymbol{u}$, η and λ which satisfy

$$\begin{aligned}
&\alpha\boldsymbol{u} - \nu\triangle\boldsymbol{u} - \nu\tfrac{\partial^2\boldsymbol{u}}{\partial z^2} + g\boldsymbol{\nabla}_{xy}\eta + \boldsymbol{\nabla}_{xy}\lambda = \boldsymbol{f}_u \quad \text{in } \Omega,\\
&\alpha\eta + \mathrm{div}_{xy}\int_{-h}^{\eta^*} \boldsymbol{u}\, dz = f_\eta \qquad \text{in } \omega,
\end{aligned} \tag{11}$$

under the constraints

$$\lambda(\eta - \Psi) = 0, \quad \lambda \geq 0, \quad \eta - \Psi \leq 0, \quad \text{in } \omega, \tag{12}$$

being Ψ a given function. We have set $\boldsymbol{f}_u = \alpha \boldsymbol{u}^n(\mathbf{X}^n)$ and $f_\eta = \alpha \eta^n$. The boundary conditions are

$$\begin{array}{ll} \dfrac{\partial \boldsymbol{u}}{\partial n} = 0 & \text{on } \Gamma_s \\ \boldsymbol{u} = 0 & \text{on } \Gamma_b \cup \Gamma_f. \end{array} \tag{13}$$

It may be recognised tat we are facing a classical saddle point problem which may be solved by duality techniques. For a given η and λ in $L^2(\omega)$ the first equation in (11) with boundary conditions (13) is well posed with $\boldsymbol{u} \in \boldsymbol{V} = \{\boldsymbol{v} \in [H^1(\Omega)]^2, \, \boldsymbol{v} = 0 \quad \text{on } \Gamma_b \cup \Gamma_f\}$.

More precisely, for a given $\phi \in \boldsymbol{V}'$ we indicate with $\boldsymbol{y} = \mathcal{F}(z)$ the element of $\boldsymbol{V}$ which satisfies (in the sense of distribution) the equation

$$\alpha \boldsymbol{y} - \nu \triangle \boldsymbol{y} - \nu \frac{\partial^2 \boldsymbol{y}}{\partial z^2} = \boldsymbol{f}_u + \phi$$

in Ω, with boundary condition $\frac{\partial \boldsymbol{y}}{\partial n} = 0$ on Γ_s. The map $\mathcal{F}$ is an isomorphism between $\boldsymbol{V}'$ and $\boldsymbol{V}$. Therefore, (11) may be formally written in the equivalent form

$$\alpha \eta + \mathrm{div}_{xy} \int_{-h}^{\eta^*} \mathcal{F}^{-1}(-g \boldsymbol{\nabla}_{xy} \eta - \boldsymbol{\nabla}_{xy} \lambda) \, dz = f_\eta, \quad \text{in } \omega, \tag{14}$$

which, for a given λ, provides an equation for η only. It may be verified that (14) is in fact akin to a wave equation for η and efficient numerical solution strategies may be devised for it [11]. We are now ready to state the Uzawa algorithm for our constrained problem.

For a given $\epsilon > 0$, $\rho > 0$ and $\lambda^{(0)} \in L^2(\omega)$, with $\lambda^{(0)} \geq 0$, solve

$$\alpha \eta^{(k+1)} + \mathrm{div}_{xy} \int_{-h}^{\eta^*} \mathcal{F}^{-1}(-g \boldsymbol{\nabla}_{xy} \eta^{(k+1)} - \boldsymbol{\nabla}_{xy} \lambda^{(k)}) \, dz = f_\eta, \quad \text{in } \omega,$$

and set

$$\lambda^{(k+1)} = \max(\lambda^{(k)} + \rho(\eta^{(k+1)} - \Psi), 0),$$

for $k = 0, 1, \ldots$, until $||\lambda^{(k+1)} - \lambda^{(k)}||_{L^2(\omega)} \leq \epsilon$.

The final iterate is used for the approximation of $\tilde{\boldsymbol{u}}$, λ^{n+1} and η^{n+1}. Finally, we either perform the full correction step (10), or, if we are making the hydrostatic assumption, we just compute the new w using the second equation in (10).

2.3 The model for the dynamics of a rowing scull

To compute the boat dynamics we need to couple between the fluid solver with and an algorithm for the structural dynamics.

Here the boat is modelled as a rigid body and following [1, 2] we have considered two orthogonal Cartesian reference frames. The inertial reference system $(\boldsymbol{O}, x, y, z)$ and a body-fixed reference system $(\boldsymbol{S}, x^b, y^b, z^b)$, whose origin is the boat centre of mass $\boldsymbol{S}$, which translates and rotates with the boat. The xy plane in the inertial reference system is parallel to the undisturbed water surface and the $z-$axis points upward. The body-fixed x^b-axis is directed from bow to stern and y^b is positive starboard.

The dynamics of the boat in the 6 degrees of freedom is described by the equations of linear and angular momentum, which in the inertial reference frame are given by

$$M\ddot{\boldsymbol{S}} = \boldsymbol{F} \tag{15}$$

and

$$\mathcal{R}\mathcal{I}\mathcal{R}^{-1}\dot{\boldsymbol{\Phi}} + \boldsymbol{\Phi} \times \mathcal{R}\mathcal{I}\mathcal{R}^{-1}\boldsymbol{\Phi} = \boldsymbol{M}_G, \tag{16}$$

respectively. Here, M is the boat mass, $\ddot{\boldsymbol{S}}$ is the linear acceleration of the centre of mass, $\boldsymbol{F}$ is the resultant of the external forces acting on the boat, $\dot{\boldsymbol{\Phi}}$ and $\boldsymbol{\Phi}$ are the angular acceleration and velocity, respectively. Finally, $\boldsymbol{M}_G$ is the moment with respect to G acting on the boat, $\mathcal{I}$ is the tensor of inertia of the boat about the body-fixed reference system axes and $\mathcal{R} = \mathcal{R}(\boldsymbol{\Phi})$ is the transformation matrix between the body-fixed and the inertial reference system (see [1] for details).

We here consider the application of the model to the dynamics of a rowing scull. A scull is a competition rowing boat where the oarsmen (also called scullers) hold both left and right oars and act on them synchronously, see Figure 3. The problem is made difficult by the strong unsteadiness of

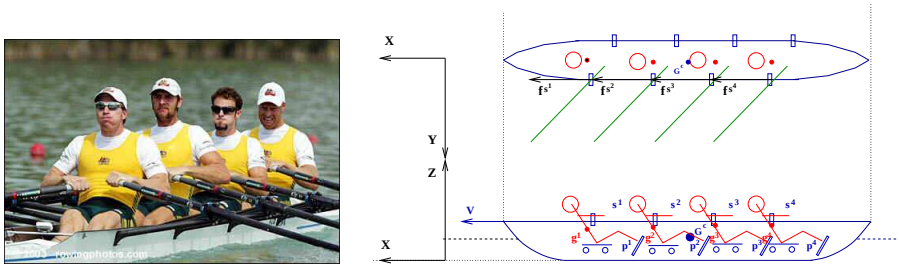

Figure 3: An actual scull (coaxless quad) on the left and its model on the right

the motion and the interaction with the free surface. Indeed, the varying forces at the oars and, even more importantly, the inertial forces due to the movement of the rowers (who slide over the boat during the rowing action)

superimpose to the mean motion a complex system of secondary movements. The latter induce an additional drag, mainly because of the gravitational waves radiating from the boat. Their account can be useful during the design process of a new boat and to understand the effects of different rowing styles or crew composition.

Because of the characteristics of a scull, we can assume as a first approximation that the motion takes place in the xy plane. This implies a great simplification of (16), which reduces to a scalar equation, being $\mathbf{\Phi} = \phi \mathbf{e}_y$.

The data we have usually available are the forces at the oarlocks $\boldsymbol{F}_{o_j}$, inferred from measurements taken on rowing machines, and the movement of the rowers. Here, j runs over the number of rowers. The latter can be extracted from a kinematic model of the rower and measurements taken using video imaging techniques[12], and is usually given as the position $\boldsymbol{g}_{ij} = \boldsymbol{g}_{ij}(t)$ of the centre of mass in the boat reference frame of portions of the body of the athlete (e.g. arm, forearm, legs, etc.), with corresponding mass m_{ij} (usually taken from anatomic tables as function of the sex, age and weight of the athlete). Here i runs over the number of parts into which the body has been subdivided. If we consider the system formed by the boat and the rowers, we need to provide the force exerted by the rowers on the oar as well, in the following indicated by $\boldsymbol{F}_{h_j}$. This force can be easily computed using a model of the oar action, therefore it is here assumed as given. We omit all details of the derivation of the model, which is rather standard and can be found in [7], and we provide only the final result. Let us indicate with

$$\mathcal{R} = \begin{bmatrix} \cos\phi & 0 & -\sin\phi \\ 0 & 1 & 0 \\ \sin\phi & 0 & \cos\phi \end{bmatrix}, \qquad \mathcal{O} = \begin{bmatrix} -\sin\phi & 0 & -\cos\phi \\ 0 & 1 & 0 \\ \cos\phi & 0 & -\sin\phi \end{bmatrix}.$$

the rotation matrix and its derivative w.r.t. ϕ, and with M the mass of the boat. We have that

$$\begin{aligned} &(M + \sum_{i,j} m_{ij})\ddot{\boldsymbol{S}} + \mathcal{O}(\sum_{i,j} m_{ij}\boldsymbol{g}_{ij})\ddot{\phi} + \mathcal{R}\sum_{j,j} m_{ij}\ddot{\boldsymbol{g}}_{ij} + 2\mathcal{O}(\sum_{i,j} m_{ij}\dot{\boldsymbol{g}}_{ij})\dot{\phi} \\ &- \mathcal{R}(\sum_{i,j} m_{ij}\boldsymbol{g}_{ij})\dot{\phi}^2 = \sum_{j=1}^{n} \boldsymbol{F}_{o_j} + \sum_{j=1}^{n} \boldsymbol{F}_{h_j} + (M + \sum_{i,j} m_{ij})\boldsymbol{g} + \boldsymbol{F}_{\text{Flow}} \quad (17a) \end{aligned}$$

and

$$\mathcal{R}(\sum_{i,j} m_{ij}\boldsymbol{g}_{ij}) \times \ddot{\boldsymbol{S}} + (I_{YY} + \sum_{i,j} m_{ij}|\boldsymbol{g}_{ij}|^2)\ddot{\phi} \tag{17b}$$
$$+ 2(\sum_{i,j} m_{ij}\mathcal{R}\boldsymbol{g}_{ij} \times \mathcal{O}\dot{\boldsymbol{g}}_{ij})\dot{\phi} = -\mathcal{R}\sum_{i,j} m_{ij}\boldsymbol{g}_{ij} \times \mathcal{R}\ddot{\boldsymbol{g}}_{ij}$$
$$+ \mathcal{R}\sum_{j=1}^{n} \boldsymbol{g}_{s_j} \times \boldsymbol{F}_{s_j} + \mathcal{R}\sum_{j=1}^{n} \boldsymbol{g}_{m_j} \times \boldsymbol{F}_{m_j} \mathcal{R}\sum_{i,j} m_{ij}\boldsymbol{g}_{ij} \times \boldsymbol{g} + \boldsymbol{M}_{\text{Flow}},$$

where the indexes i and j run from the number of body parts and the number of rowers, respectively. The dependence on t of the various terms is understood.

Equations (17) form a system of three nonlinear second order ordinary differential equations in the variables (S_x, S_z, ϕ), that must be complemented with a suitable fluid dynamic model in order to compute $\boldsymbol{F}_{\text{Flow}}$ and M_{Flow} and close the problem. For instance, the model proposed in the previous sections.

2.4 More realistic boundary conditions

We need to make the boundary conditions on Γ_b and Γ_f more realistic. On the bottom, we normally prescribe a friction condition through a Chézy coefficient c_d. Being the bottom flat it corresponds on setting

$$w = 0 \qquad \nu\frac{\partial \boldsymbol{u}}{\partial z} = c_d|\boldsymbol{u}|\boldsymbol{u}, \quad \text{on } \Gamma_b,$$

the non-linear term in the right-hand side being discretized in time in a semi-explicit fashion. On the far field, we employ a first order linear radiation condition for the elevation, i.e. we impose

$$\frac{\partial \eta}{\partial t} + \sqrt{gh}\frac{\partial \eta}{\partial n} = 0, \quad \text{on}\Gamma_f(t),$$

which is approximated by using an extrapolation technique akin to the characteristic treatment of the time-derivative already illustrated. The modifications to the numerical scheme are straightforward.

3 The interaction between the boat and the water

The scull dynamic model and the flow model have to interact. In particular the forces $\boldsymbol{F}_{\text{Flow}}$ and the angular momentum $\boldsymbol{M}_{\text{Flow}}$ acting on the boat depend on the flow solution. However, the dynamic condition (4) implies a zero tangential component of the normal stresses on the boat surface, while the normal component is simply given by λ. Therefore, the proposed fluid

dynamics model is able to compute correctly pressure induced forces, but neglects the viscous drag. Yet, for elongated geometries like a scull the viscous drag $\boldsymbol{F}_D(\boldsymbol{U}) = -R(\boldsymbol{U})\mathbf{e}_x$[1] can be estimated by standard empirical formula, which are quite accurate. Therefore, we may write that

$$\boldsymbol{F}_{\text{Flow}} = \int_{\Gamma_\Psi} \lambda \boldsymbol{n} d\gamma + \boldsymbol{F}_D(\boldsymbol{U}) = \int_\omega \lambda \left[\frac{\partial \Psi}{\partial x}, \frac{\partial \Psi}{\partial x}, 1\right]^T dxdy + \boldsymbol{F}_D(\boldsymbol{U}).$$

We have here exploited the fact that the normal the surface Γ_Ψ is given by $\boldsymbol{n} = (\sqrt{1 + |\boldsymbol{\nabla}_{xy}\Psi|^2})^{-1}[\frac{\partial \Psi}{\partial x}, \frac{\partial \Psi}{\partial y}, 1]^T$ and, for the sake of completeness we have given the general formula, while in the case of a scull the y component of $\boldsymbol{F}_{\text{Flow}}$ is zero because of symmetry considerations. An analogous formula may be obtained for the computation of the couple $\boldsymbol{M}_{\text{Flow}}$ induced by the action of the flow. We have also implicitly used the fact that $\lambda = 0$ outside the area where the boat is present.

The boat dynamical system describes the position of the boat and thus implicitly defines the function Ψ. Let $\mathcal{B}_0 = \{(x^b, y^b, z^b), \quad (x^b, y^b) \in B \subset \mathbb{R}^2, z^b = \hat{r}_0^b(x^b, y^b)\}$ be the parametric description of the boat external surface (the skin) in the boat reference frame, usually provided by means of analytic functions. We first extend $\hat{r}^b$ with continuity to the whole $\mathbb{R}^2$ in a suitable way, and let $\hat{r}^b$ indicate this extension. The extended boat geometry at time t can then be described as $\mathcal{B}(t) = \{(x, y, z), \quad (x, y)\mathbb{R}^2,\ z = r(x, y, t))$ where

$$r(x, y, t) = S_z(t) + \tan\phi(t)[x - S_x(t)] + \cos^{-1}\phi(t)\hat{r}^b(\mathcal{R}(\phi(t))[\boldsymbol{x} - \boldsymbol{S}(t)]).$$

Finally, Ψ can be taken as r restricted to ω.

4 Numerical results

When considering the dynamics of the scull, the value of Ψ at each time step is given by solving equations (17), where the hydrodynamic forces are computed by integrating the surface stress provided by the Navier-Stokes model just presented.

For the space discretisation we have adopted a finite element scheme which employs Raviart-Thomas $\mathbb{RT}_0$ triangular elements in the (x, y) plane for $\boldsymbol{u}$ and standard P^1 elements for w. The elevation η, as well as the multiplier λ, is approximated by a piecewise constant function (i.e. P_0 finite elements). Details are given in [11].

We have implemented a simple time integration procedure of the coupled problem. We evolve from time step t^n to t^{n+1} as follows:

- the body position is integrated explicitly using the fluid dynamic forces $\boldsymbol{F}^n_{\text{Flow}}$ and $\boldsymbol{M}^n_{\text{Flow}}$ computed from the flow solution at time stem t^n;

[1] In fact the drag is also a function of the submerged surface.

Length $[m]$	Breadth $[m]$	Height $[m]$	Mass $[kg]$	$\mathcal{I}_{yy}$ $[kg\,m^2]$
6	0.8	0.6	400	930

- once the approximation Ψ^{n+1} of the constraining surface is available, we solve the fluid dynamic problem using the Uzawa algorithm;
- once η^{n+1}, λ^{n+1}, and $\boldsymbol{U}^{n+1}$ have been obtained we move to the next time step.

This explicit scheme is subject to an absolute stability condition. Yet, the time steps required to capture the rather fast dynamics of the generated waves has been found to be within the stability bounds, at least for the computations carried out so far.

The numerical results presented in the following section have been obtained using the hydrostatic assumption *i.e.* the flow solution is computed neglecting the hydrodynamic pressure term q.

4.1 Sinking and pitching motions

For all the following dynamic simulation the scull has been approximated by a semi-ellipsoid. Its geometric, mass and inertia characteristics are summarised in table 4.1.

The first simulation is a pure sinking motion: the hull is free to move in the z direction subject to its weight. The initial position is at the centre of a square basin of edge length $15m$. At time $t = 0$ the body is steady at $z = 0.6m$ over the free surface. The motion, represented in figure is a sequence of damped oscillations and after a few seconds the vertical position levels off at $z = 0.30m$. The asymptotic sinking is in good agreement with the theoretical equilibrium position of $z = 0.325m$.

Pure pitching motion was also simulated: vertical position was fixed and a non-zero initial pitch angle $\theta_0 = 1.5^\circ$ was assigned. As in the sinking motion, oscillations damps out and pitch angle tends to its zero equilibrium value. Damping is considerably lower compared to the previous simulation, due to the smaller wave amplitude generated. This is also in accordance to experience. Figures 4 represents the wave pattern generated by sinking and pitching motion, respectively (beware: colour scales are different).

4.2 Reproducing mean motion wave pattern

A further test concerns the wave pattern generated by the advancing motion on free surface. In *shallow water* regime, i.e. for $H < 2v^2/g$, theory predicts for bow and stern waves a semi-angle $\beta = \operatorname{asin}\left(\frac{c}{v}\right)$ where the wave speed c is constant in the hydrostatic assumption and equal to $\sqrt{gh}$ (see [10]). Setting $h = 3m$ this angle turns out to be 64.7°.

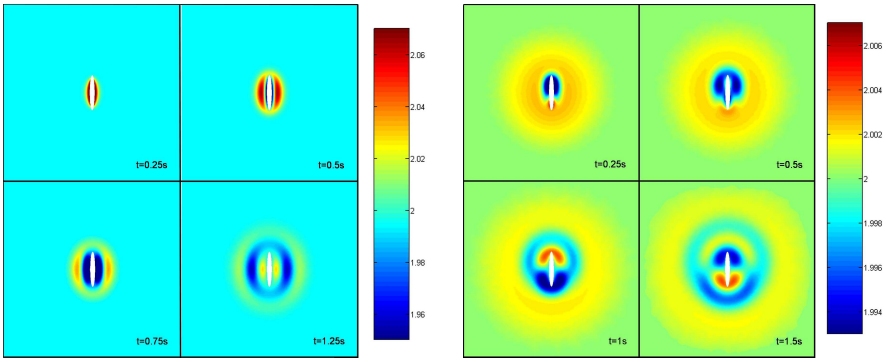

Figure 4: Wave pattern for sinking (left) and pitching motion (right)

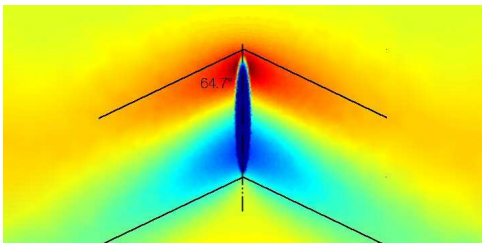

Figure 5: The wave pattern generated and its expected angle

In figure 5 the predicted angle is overlaid on the calculated wave pattern (colour scale is proportional to free surface elevation). The agreement is satisfactory demonstrating the effectiveness of the procedure.

4.3 An example with the full dynamics

We have here considered a coaxless quad scull. The first picture in Fig. 6 illustrates the wave pattern generated by the boat moving at the constant mean velocity, computed using the model given in Section 2. The second and third pictures illustrate that obtained at the instant of the catch and at the release, when the full dynamics of the boat is considered. We have assumed a stroke period of 1.5 seconds.

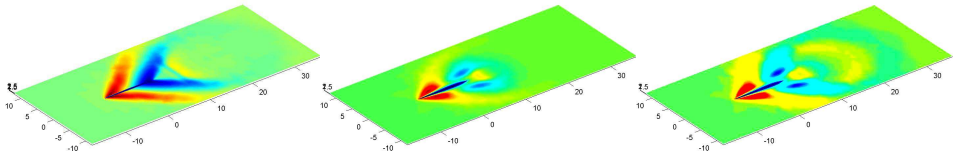

Figure 6: The surface wave pattern for the mean motion (left) and at two different time instants obtained using the full boat dynamics

The alteration to the wave pattern caused by the secondary motions is evident. Comparison with experimental data is currently under way. So far, we have carried out only qualitative assessment comparing the wave pattern with that obtained from video recording, with good agreement.

4.4 A final detail

The numerical model described so far has a practical disadvantage. As the boat moves it will eventually reach the boundary of the computational domain. As a consequence, to simulate the boat during a race for reasonably long periods we may need a rather large ω, with an increase in the computational costs. We have successfully overcome this problem by re-writing the flow equations in a non-inertial reference system with origin on the boat centre of mass $\boldsymbol{S}$, and axis directions kept fixed. What is needed is the addition of the inertial forces and some changes in the boundary conditions in the flow equations. In this way the variations in γ_Ψ are only due to the sinking and pitching motion, while the boat centre remains fixed. For the sake of brevity we have not reported here the modified equations even if the last computations here shown have been indeed computed this way.

5 Acknowledgements

The authors wish to thank Filippi Lido s.r.l for the financial and technical support and in particular Ing. Alessandro Placido for having introduced them to the wonderful world of rowing. A thank also to Andrea Paradiso for making available some results from his master theses.

The authors want to remember the late Fausto Saleri, who has largely contributed to the development of some of the ideas here illustrated, before leaving us untimely.

References

[1] R. Azcueta. Computation of turbulent free-surface flows around ships and floating bodies. *Ship Technology Research*, 49(2):46–69, 2002.

[2] R. Azcueta. RANSE Simulations for Sailing Yachts Including Dynamic Sinkage & Trim and Unsteady Motions in Waves. In *High Performance Yacht Design Conference*, pages 13–20, Auckland, 2002.

[3] K. Boukir, Y. Maday, B. Métivet, and E. Razafindrakoto. A high-order characteristics/finite element method for the incompressible Navier-Stokes equations. *Internat. J. Numer. Methods Fluids*, 25(12):1421–1454, 1997.

[4] U. P. Bulgarelli. The application of numerical methods for the solution of some problems in free-surface hydrodynamics. *Journal of Ship Research*, 49(4):288–301, 2005.

[5] U. P. Bulgarelli, C. Lugni, and M. Landrini. Numerical modelling of free-surface flows in ship hydrodynamics. *Int. Journal Num. Meth. Fluids*, 43(5):465–481, 2003.

[6] A.J. Chorin. Numerical solution of the Navier Stokes equations. *Math. Comp.*, 22:745–762, 1968.

[7] L. Formaggia, E. Miglio, A. Mola, and N. Parolini. Fluid-structure interaction problems in free surface flows: application to boat dynamics. *Int. Journal Num. Meth. Fluids*, 2007. DOI 10.1002/fld.1583 (in press).

[8] J. L. Lions, R. Temam, and S. Wang. On the equations of the large-scale ocean. *Nonlinearity*, 5:1007–1053, 1992.

[9] J. L. Lions, R. Temam, and S. Wang. On mathematical problems for the primitive equations of the ocean: the mesoscale midlatitude case. *Nonlinear Anal.*, 40:439–482, 2000.

[10] C.C. Mei. *The applied dynamics of ocean surface waves*. World Sceintific Publishing, Singapore, 1989. Second printing with corrections.

[11] E. Miglio, A. Quarteroni, and F. Saleri. Finite element approximation of quasi-3D shallow water equations. *Comp. Meth. Appl. Mech. Engng.*, 174(3-4):355–369, 1999.

[12] A. Mola, L Formaggia, and E. Miglio. Simulation of the dynamics of an olympic rowing boat. In *Proceedings of ECCOMAS CFD 2006,Egmond aan Zee, September 5-8, The Netherlands*. TU Delft, 2006. ISBN: 90-9020970-0.

[13] H. Orihara and H. Miyata. Evaluation of added resistance in regular incident waves by computational fluid dynamics motion simulation using an overlapping grid system. *Journal of Marine Science and Technology*, 8(2):47–60, 2003.

[14] N. Parolini and A. Quarteroni. Mathematical models and numerical simulations for the America's Cup. *Comp. Meth. Appl. Mech. Engng.*, 194(9-11):1001–1026, 2005.

[15] N. Parolini and A. Quarteroni. Modelling and numerical simulation for yacht design. In *Proceedings of the 26th Symposium on Naval Hydrodynamics, Rome, Italy, 17-22 September 2006*, 2007. To appear.

[16] C. Yang and R. Lohner. Calculation of ship sinkage and trim using a finite element method and unstructured grids. *International Journal of Computational Fluid Dynamics*, 16(3):217–227, 2002.

MOX Technical Reports, last issues

Dipartimento di Matematica "F. Brioschi",
Politecnico di Milano, Via Bonardi 9 - 20133 Milano (Italy)

16/2008 L. Formaggia, E. Miglio, A. Mola, A. Scotti:
Numerical simulation of the dynamics of boat by a variational inequality approach

15/2008 S. Micheletti, S. Perotto:
An anisotropic mesh adaptation procedure for an optimal control problem of the advection-diffusion-reaction equation

14/2008 C. D'Angelo, P. Zunino:
A finite element method based on weighted interior penalties for heterogeneous incompressible flows

13/2008 L.M. Sangalli, P. Secchi, S. Vantini, V. Vitelli:
K-means alignment for curve clustering

12/2008 T. Passerini, M.R. de Luca, L. Formaggia, A. Quarteroni, A. Veneziani:
A 3D/1D geometrical multiscale model of cerebral vasculature

11/2008 L. Gerardo Giorda, L. Mirabella, F. Nobile, M. Perego, A. Veneziani:
A model preconditioner for the Bidomain problem in electrocardiology

10/2008 N. Grieco, E. Corrada, G. Sesana, G. Fontana, F. Lombardi, F. Ieva, A.M. Paganoni, M. Marzegalli:
Predictors of the reduction of treatment time for ST-segment elevation myocardial infarction in a complex urban reality. The MoMi^2 survey

9/2008 P. Secchi, E. Zio, F. Di Maio:
Quantifying Uncertainties in the Estimation of Safety Parameters by Using Bootstrapped Artificial Neural Networks

8/2008 S. Micheletti, S. Perotto:
Space-time adaptation for purely diffusion problems in an anisotropic framework

7/2008 C. Vergara, R. Ponzini, A. Veneziani, A. Redaelli, D. Neglia, O. Parodi:
Reliable CFD-based Estimation of Flow Rate in Hemodynamics Measures. Part II: Sensitivity Analysis and First Clinical Application